Citation: BoneKEy Reports **5**, Article number: 804 (2016) | doi:10.1038/bonekey.2016.31

www.nature.com/bonekey

LABORATORY METHODS

Murine models of breast cancer bone metastasis

Laura E Wright[1], Penelope D Ottewell[2], Nadia Rucci[3], Olivier Peyruchaud[4], Gabriel M Pagnotti[5], Antonella Chiechi[1], Jeroen T Buijs[6] and Julie A Sterling[7,8]

[1]Division of Endocrinology, Department of Medicine, Indiana University, Indianapolis, IN, USA. [2]Department of Oncology, Mellanby Center for Bone Research, University of Sheffield, Sheffield, UK. [3]Department of Biotechnological and Applied Clinical Sciences, University of L'Aquila, L'Aquila, Italy. [4]Physiopathologie, Diagnostic et Traitements des Maladies Osseuses, INSERM, UMR_S1033, Lyon, France. [5]Department of Biomedical Engineering, Stony Brook University, Stony Brook, NY, USA. [6]Department of Thrombosis & Hemostasis, Leiden University Medical Center, Leiden, The Netherlands. [7]Department of Medicine, Division of Clinical Pharmacology, Vanderbilt University, Nashville, TN, USA. [8]Department of Veterans Affairs, Tennessee Valley Healthcare System, Nashville, TN, USA.

Bone metastases cause significant morbidity and mortality in late-stage breast cancer patients and are currently considered incurable. Investigators rely on translational models to better understand the pathogenesis of skeletal complications of malignancy in order to identify therapeutic targets that may ultimately prevent and treat solid tumor metastasis to bone. Many experimental models of breast cancer bone metastases are in use today, each with its own caveats. In this methods review, we characterize the bone phenotype of commonly utilized human- and murine-derived breast cell lines that elicit osteoblastic and/or osteolytic destruction of bone in mice and report methods for optimizing tumor-take in murine models of bone metastasis. We then provide protocols for four of the most common xenograft and syngeneic inoculation routes for modeling breast cancer metastasis to the skeleton in mice, including the intra-cardiac, intra-arterial, orthotopic and intra-tibial methods of tumor cell injection. Recommendations for *in vivo* and *ex vivo* assessment of tumor progression and bone destruction are provided, followed by discussion of the strengths and limitations of the available tools and translational models that aid investigators in the study of breast cancer metastasis to bone.

BoneKEy Reports **5**, Article number: 804 (2016) | doi:10.1038/bonekey.2016.31

Introduction

Breast cancer metastasis to the skeleton and subsequent bone destruction often result in severe bone pain, fragility fractures, nerve compression syndromes and hypercalcemia of malignancy resulting in significant morbidity and mortality.[1,2] Elucidation of the molecular mechanisms that mediate breast cancer bone metastases and cancer-induced bone destruction has begun to reveal potential therapeutic targets that may lead to improved patient survival and quality of life; however, further investigation is necessary to address this currently irreversible late-stage complication of malignancy. Therefore, it is of utmost importance for investigators to establish well-characterized *in vivo* models of breast cancer bone metastasis.

Unlike the study of postmenopausal osteoporosis where the ovariectomy model is the clear FDA-mandated choice,[3] there are numerous murine models of breast cancer metastasis to bone, each with its own benefits and limitations. Because spontaneous metastasis to the skeleton from primary tumors in animals is rare,[2] and no single model reproduces all of the genetic and phenotypic changes of human breast cancer bone metastasis, researchers must select a model or a combination of models that best suits the aspect of the metastatic disease that they wish to investigate. Here we (1) identify the most commonly utilized breast cancer cell lines that elicit osteolytic, osteoblastic or mixed phenotypes in bone, (2) provide protocols for tumor cell inoculation routes that model metastatic disease in the skeleton and (3) explore methods for the post-inoculation monitoring of breast cancer progression in bone.

Modeling osteolytic breast cancer bone metastases

Inoculation of bone trophic tumor cells directly into the blood stream provides a useful tool for investigating the processes associated with breast cancer cell homing, colonization and subsequent metastatic tumor growth and osteolytic lesion

Correspondence: Dr LE Wright, Division of Endocrinology, Department of Medicine, Indiana University, 980 West Walnut Street Walther Hall R3, Room C132, Indianapolis, IN 46202, USA.
E-mail: laewrig@iu.edu

Received 21 October 2015; accepted 2 April 2016; published online 11 May 2016

formation in bone. Intra-cardiac inoculation of human triple negative MDA-MB-231 adenocarcinoma cells into immune-compromised mice (i.e., BALB/c nude, MF1 nude and NOD/SCID) results in tumor cell dissemination through the arterial vascular system and homing primarily to long bones, spine, jaw and lungs (**Figure 1a**; **Table 1**).[4,5] In syngeneic tumor models where murine-derived cell lines are inoculated into a murine host, a bone metastatic profile can be observed with varying degrees of success following intra-cardiac injection of 4T1 or PyMT MMTV mammary cancer cells into immune competent BALB/c or FVB/N mice, respectively (**Table 1**).[6,7]

Visceral metastases, particularly to the lung, can significantly shorten the life span of a mouse and thus limit the experimental time frame during which skeletal metastases can be studied *in vivo*. MDA-MB-231 and 4T1 cell lines have therefore been manipulated in the laboratory to produce bone-seeking sub-lines that favor homing to and colonization of mouse tibiae and femurs with a reduced propensity to metastasize to the lung. Bone-seeking sub-lines, often referred to in the literature as MDA-MB-231-B02, MDA-MB-231-1833, MDA-MB-231-B, MDA-IV and MDA-MB-231-bone, form tumors in the long bones of up to 90% of mice following intra-cardiac inoculation in BALB/c nude mice.[8–12] Intra-cardiac inoculation of the subline 4T1-2 cells into BALB/c mice results in bone metastases in 70–80% of animals (**Table 1**).[13]

Direct intra-tibial injection of a number of breast cancer cell lines including MDA-MB-231, MDA-MB-436 and SUM1315 into immunocompromised mice and 4T1 and PyMT MMTV cell lines into immune competent BALB/c and FVB/N mice results in the development of osteolytic mammary tumors in bone with minimal impact outside of bone marrow engraftment (**Figure 1b**; **Table 1**).[7,14,15] The intra-tibial model bypasses the early stages of metastasis including homing to the bone microenvironment and is therefore useful for a more direct assessment of tumor–bone interactions, particularly when interested in studying genetic manipulations of the host or tumor cells of interest.

Intra-cardiac, intra-arterial and intra-tibial inoculation of cancer cells provide useful tools for examining the later stages of breast cancer bone metastasis; however, these aforementioned models do not permit investigation into the stages that precede the colonization of breast cancer in bone, including primary tumor growth or the dissemination of tumor cells through intravazation. The 4T1 mouse mammary cancer cell line was derived from a BALB/c spontaneous mammary carcinoma,[16] and orthotopic inoculation of 4T1 cells into the

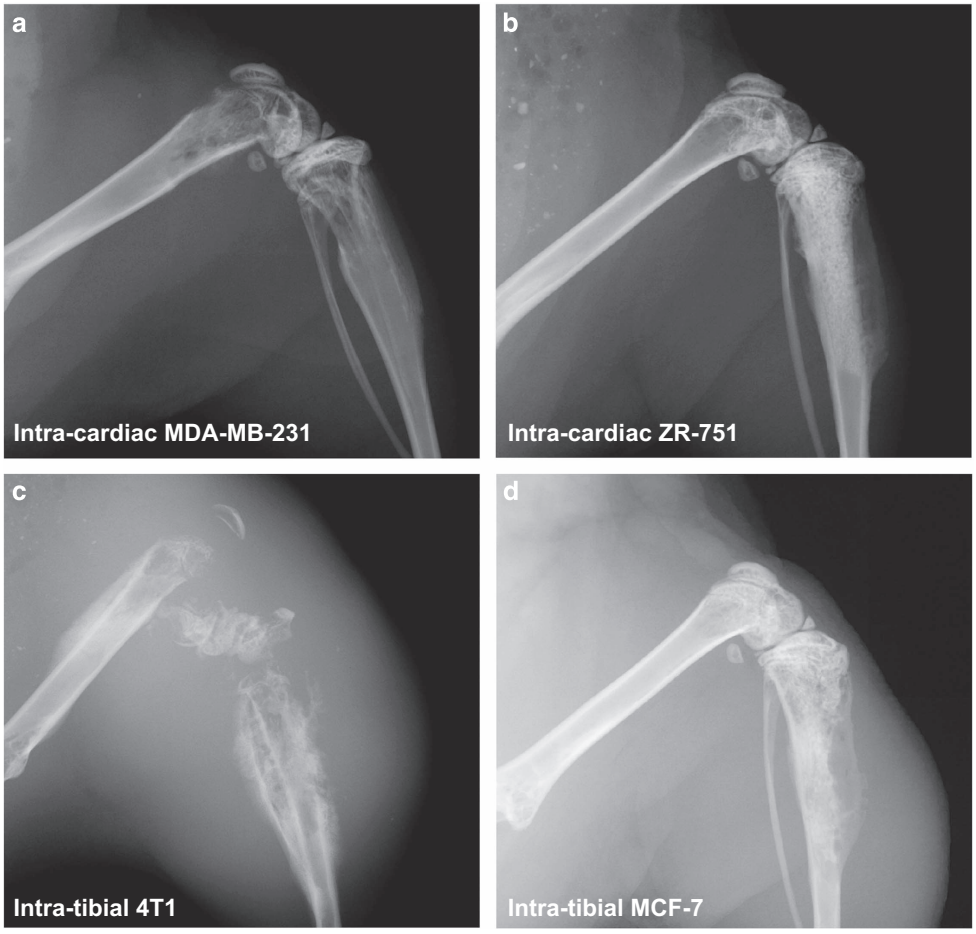

Figure 1 Radiographs of the distal femur and proximal tibia of mice with breast cancer bone metastases. Representative images are presented of (**a**). MDA-MB-231 breast cancer bone metastases 4 weeks post inoculation of 100 000 cells via intra-cardiac route, (**b**). ZR-75-1 breast cancer bone metastases 25 weeks post inoculation of 100 000 cells via intra-cardiac route, (**c**). 4T1 breast cancer bone metastases 4 weeks post inoculation of 10 000 cells via intra-tibial route, and (**d**). MCF-7 breast cancer bone metastases 20 weeks post inoculation of 100 000 cells via intra-tibial route.

Table 1 Human and mouse mammary cancer cell lines that form osteolytic bone lesions following inoculation into mice

Cell line	*Species*	*Origin*	*Subline*	*Mouse strain*	*Inoculation route*	*Metastatic site(s)*	*Time to lesion formation*
MDA-MB-231	Human	Human mammary adenocarcinoma isolated from a pleural effusion from a 51-year-old Caucasian female	Parental	BALB/c nude MF1 nude NOD/SCID NSG	Intra-cardiac Intra-tibial Orthotopic	Mouse long bones, spine and jaw Mouse tibiae Mouse bones	2–3 weeks 1–3 weeks 7 weeks
			MDA-MB-231-BO2	BALB/c nude	Intra-cardiac Intra-tibial Intra-arterial	Mouse long bones, spine and jaw Mouse tibiae Mouse long bones	2–3 weeks 1–3 weeks 2–3 weeks
			MDA-MB-231-IV	BALB/c nude	Intra-cardiac Intra-tibial Intra-arterial Intra-venous Orthotopic	Mouse long bones, spine and jaw Mouse tibiae Mouse long bones Mouse long bones Human bone X-plants	2–3 weeks 1–3 weeks 2–3 weeks 2–3 weeks 10–14 weeks
MDA-MB-436	Human	Human mammary adenocarcinoma isolated from a pleural effusion from a 43-year-old Caucasian female	Parental	MF1 nude BALB/c nude NOD/SCID	Intra-osseous	Mouse tibiae	2–3 weeks
SUM1315	Human	Isolated from a metastatic nodule of a Caucasian female patient with ductal carcinoma	Parental	NOD/SCID	Intra-tibial Orthotopic	Mouse tibiae Human bone X-plants	3–4 weeks 8–12 weeks
4T1	Mouse	Isolated from a stage 1 V mammary tumor from a female BALB/c cfC3H mouse	Parental	BALB/c cfC3H	Intra-cardiac Intra-tibial Orthotopic	Mouse long bones, spine, jaw and lungs Mouse tibiae Mouse long bones, jaw and lungs	2–3 weeks 1–3 weeks 3–6 weeks
			4T1-2	BALB/c cfC3H	Intra-cardiac Intra-tibial Orthotopic	Mouse long bones, spine, jaw and lungs Mouse tibiae Mouse long bones, jaw and lungs	2–3 weeks 1–3 weeks 3–4 weeks
PyMT MMTV	Mouse	Isolated from mammary tumour induced by MMTV viral oncogene in FVB/N female mouse	Parental	FVB/N	Intra-cardiac Intra-tibial	Mouse long bones, spine, jaw and lungs Mouse tibiae	2–3 weeks 1–2 weeks
KEP	Mouse	Mouse invasive lobular carcinoma derived from a Keratin14-driven E-cadherin/p53 (KEP) knock out primary mammary carcinoma	KEP/Luc KEP/Luc	$RAG^{-/-}$; $IL2R\gamma c^{-/-}$ BALB/c BALB/c nude	Orthotopic Intra-cardiac Orthotopic Intra-tibial	Spine Mouse long bones and spine Mouse long bones and spine Mouse tibiae	3–5 weeks 2–4 weeks 6–9 weeks 2–4 weeks

mammary fat pad of BALB/c mice results in spontaneous metastasis to lungs (~60% of mice) and bone (~20–30% of mice; **Table 1**).[17] Incidence of bone metastasis can be increased to 50–70% by utilizing the bone-seeking 4T1-2 subline.[18,19] This syngeneic model has the benefit of utilizing an immune competent mouse.

Recently, it was shown that orthotopic inoculation of luciferase-transduced murine invasive lobular breast carcinoma cells (KEP cells) resulted in the formation of bone metastases in the appendicular and axial skeleton within 3 weeks after resection of the orthotopic tumor with minimal lung involvement in BALBc nude mice (**Table 1**).[20] Although MDA-MB-231 do not metastasize to murine bone from the orthotopic site in BALB/c nude and NOD SCID mice, distant metastases at skeletal sites were observed when using NSG mice,[21] suggesting the importance of NK cells in regulating the metastatic process.

Spontaneous metastasis of an orthotopic human breast cancer tumor to bone can be achieved in an immune-compromised mouse using a unique model that incorporates human-derived bone X-plants. In recent studies, orthotopic inoculation of human-derived SUM-1315 or MDA-MB-231-IV cells into the mammary fat pad of NOD SCID mice 4 weeks following ectopic implantation of human bone resulted in spontaneous metastasis of human breast cancer cells specifically to the human bone grafts in 40–60% of animals (**Table 1**).[22,23]

Modeling osteoblastic breast cancer bone metastases

Although patients with breast cancer usually develop osteolytic bone metastases, as many as 25% will present with osteoblastic bone metastases.[24] The human breast cancer cell lines ZR-75-1 and MCF-7 can be utilized to establish an osteoblastic bone metastatic phenotype in mice.

ZR-75-1 cultures were initially derived from a malignant ascetic effusion in a 63-year-old Caucasian female with ductal carcinoma. ZR-75-1 cells possess receptors for all four classes of steroid hormones and are thus responsive to estradiol stimulation.[25,26] Mice inoculated via intra-cardiac route with ZR-75-1 cells develop osteoblastic bone metastases in the long bones; however, bone metastases are typically not detectable by X-ray for 12–25 weeks post inoculation (**Figure 1c**; **Table 2**).

Table 2 Human mammary cancer cell lines that form osteoblastic bone lesions following inoculation into mice

Cell line	*Species*	*Origin*	*Subline*	*Mouse strain*	*Inoculation route*	*Metastatic site(s)*	*Time to lesion formation*
MCF-7	Human	Human mammary adenocarcinoma isolated from a pleural effusion in a 69-year-old Caucasian female	Parental	BALB/c nude	Intra-cardiac Intra-tibial	Mouse long bones Mouse tibiae	20–25 weeks 1–3 weeks
			MCF-7/Neu	BALB/c nude	Intra-cardiac Intra-tibial	Mouse long bones Mouse tibiae	10–12 weeks 1–3 weeks
ZR-75-1	Human	Human ductal carcinoma derived from a malignant ascetic effusion in a 63-year-old Caucasian female	Parental	BALB/c nude	Intra-cardiac	Mouse long bones and spine	12–25 weeks

Human MCF-7 breast cancer cells were derived from a metastatic pleural effusion in a 69-year-old Caucasian female with breast carcinoma.[27] MCF-7 cells retain characteristics of differentiated mammary epithelium and possess estrogen receptors.[27,28] Intra-cardiac inoculation of MCF-7 cells in immune-compromised mice results in mixed osteolytic/osteoblastic bone metastases in the long bones after 20–25 weeks (**Table 2**). In order to speed metastatic progression, the MCF-7 cell line has been stably transfected with the oncogene Neu, and this cell line establishes mixed osteolytic and osteoblastic bone metastases in immunocompromised mice within 10–12 weeks after intra-cardiac inoculation.[29] Because ER + MCF-7 cell growth is estrogen dependent mice should be implanted subcutaneously with slow-release estradiol pellets (0.25 mg) prior to intra-cardiac tumor cell inoculation in order to more closely mimic a pre-menopausal tumor environment and speed the progression of tumor growth in bone.[30,31] MCF-7 and MCF-7/Neu cells are also commonly utilized to establish bone lesions in mice via the intra-tibial inoculation route, with lesions developing in a shorter time span of 1–3 weeks post injection (**Figure 1d**; **Table 2**). Estradiol supplementation is typically not introduced when MCF-7 cells are directly implanted into bone.

Materials and Methods

This section begins by detailing recommendations for the preparation of breast cancer cells and pre-operative care instructions for the handling of mice prior to inoculation. Four of the most commonly utilized cell inoculation routes resulting in breast cancer bone metastases are then described, including lists of necessary materials for each technique. Recommendations for the post-inoculation monitoring of animals and assessment of tumor progression in bone *in vivo* and *post mortem* are then described.

Breast cancer cell preparation

Manufacturer specifications should guide the user as to the appropriate growth conditions for the cell line of interest. As a general rule for all tumor cell inoculation routes, prepare cells from a fresh batch of low passage number. Split cells 1–2 days prior to the injections such that they reach ~80% confluence on the day of inoculation. Overcrowding of tumor cells can affect their metastatic potential *in vivo;* therefore, cell confluence prior to inoculation must be monitored judiciously. Wash flasks briefly with the appropriate cold cell culture media or phosphate-buffered saline (PBS), trypsinize (0.15% Trypsin EDTA) at 37 °C, and remove cells with ice-cold media containing 10% fetal bovine serum (FBS). Centrifuge (200 g, 5 min) and suspend the cell pellet in ice-cold PBS for quantitation. Re-suspend the cells at the desired concentration (**Table 3**) in cold PBS and keep the cell suspension for no more than 30 min on ice until the moment of inoculation. Prepare cells in small batches (enough for 1–2 cages or 5–10 animals) and keep on ice to minimize clumping and risk of embolism during the *in vivo* inoculation. Because of volumetric limitations of the mouse circulation 100 μl is the recommended injection volume using the intra-cardiac or intra-arterial routes.

Reagents for tumor cell preparation

(1) PBS (without Ca^{2+} and Mg^{2+})
(2) 0.15% Trypsin EDTA
(3) Cold Dulbecco's Modified Eagle Medium (or other media) with 10% FBS

Pre-operative management of mice

For the intra-cardiac, intra-arterial and intra-venous metastasis models, mice are inoculated between 4 and 6 weeks of age, as tumor-take is markedly reduced after 6 weeks. For the intra-tibial injection, 6- to 8-week-old mice are typically used, as tibiae of younger mice are small and difficult to inject accurately. A ketamine/xylazine cocktail (100 mg kg^{-1} and 10 mg kg^{-1}, respectively) or isoflurane (2.5% isoflurane at 2–3 l min^{-1} O_2) may be utilized for anesthesia during the inoculation of tumor cells depending on the laboratory's preference. Many groups, however, experience improved survival rates following intra-cardiac inoculation with the use of isoflurane (vs ketamine/xylazine), likely due to increased vascular tone and body temperature. If the mouse strain selected is furred, it may be important to shave the mouse at the site of inoculation for better visualization of anatomical landmarks.

Cellular inoculation routes for modeling breast cancer bone metastases in mice

Intra-cardiac inoculation of breast cancer cells. Once a mouse has been properly anesthetized and is unresponsive to pinch, place it on a sterile surface in supine position ensuring that the vertebral column is straight. Tape the forelimbs away from the torso at a slightly angled and upward position (**Figure 2a**). Prior to inoculation, clean the chest of the animal thoroughly with betadine and wipe with an alcohol pad or as per the institutional standard operating procedures. Once the chest has been sterilized, gently place one hand on the chest of the mouse to tighten the skin and mark the top of the sternum and the xyphoid process (distal sternum) with a permanent marker (**Figure 2a**). Make a third mark in the middle of these two landmarks and slightly to your right (animal's left) just over the heart in the third intercostal space (**Figure 2a**). This mark identifies the location of the left cardiac ventricle where you will insert the needle for tumor cell inoculation.

With intra-cardiac inoculation, prepare the needle by leaving a small air space in the top of the syringe before slowly drawing up the desired volume of cell suspension into the syringe (**Figure 2b**). This air space will permit a small influx of bright red oxygenated blood into the syringe hub when properly inserted into the left cardiac ventricle. Hold the skin of the mouse tight with one hand and insert the needle perpendicularly into the middle marking (**Figure 2c**). When the needle has entered the left cardiac ventricle, watch for the pulse of blood to appear in the hub of the needle. The appearance of air bubbles in the needle hub upon insertion

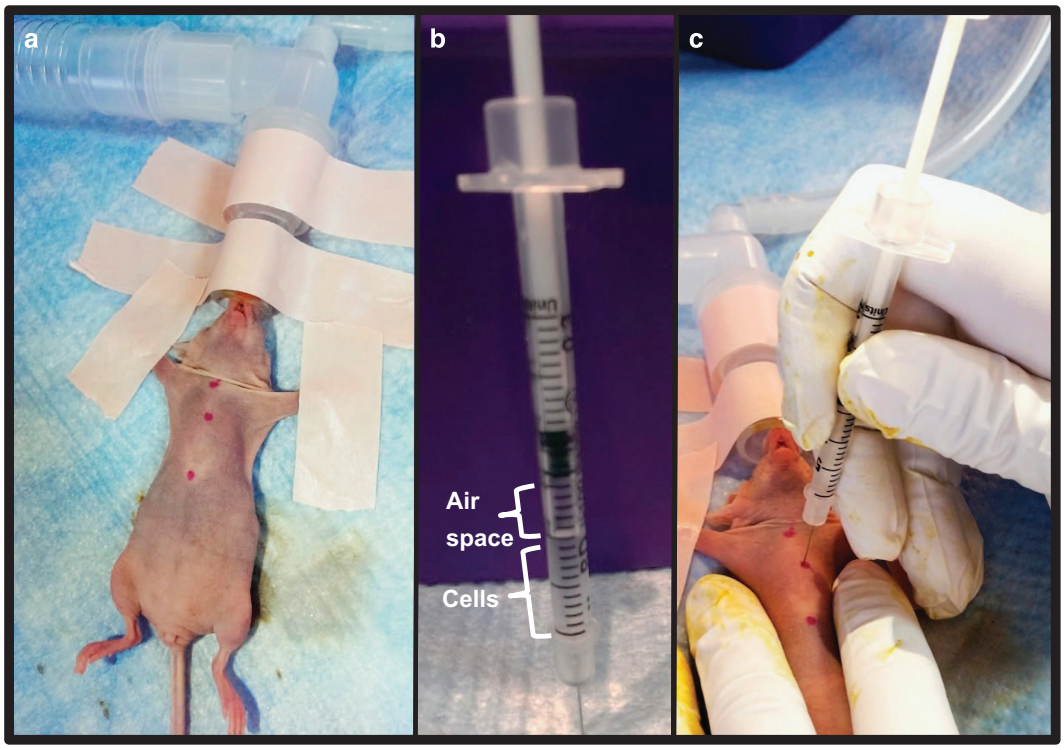

Figure 2 Inoculation of breast cancer cells in the left cardiac ventricle of a mouse. (**a**) Sterilize the chest of an anesthetized mouse and mark the top of the sternum and the xyphoid process (distal sternum) with a permanent marker. Make a 3rd mark in the middle of these two landmarks and slightly to your right (animal's left) just over the heart in the third intercostal space. (**b**) Prepare the needle by leaving a small air space in the top of the syringe before slowly drawing up the desired volume of cell suspension into the syringe. This air space will permit a small influx of bright red oxygenated blood into the syringe hub when properly inserted into the left cardiac ventricle. (**c**) Once the needle is correctly positioned in the left cardiac ventricle, inject the cell suspension slowly into the left ventricle being careful not to move the needle or press it deeper into the thoracic cavity.

indicates that it has likely entered the lungs and will need to be removed and repositioned. If you do not see a red pulse of blood in the needle hub but are confident that you are in the correct location, you can pull up slightly on the syringe plunger to verify your position in the cardiac ventricle. If there is still no visible red pulse, the needle can be slowly and slightly adjusted up or down. When small adjustments are futile, remove and reposition the insertion point completely or set the mouse aside temporarily. Extended anesthesia can cause vasoconstriction and reduce the animal's blood pressure such that the pulse of blood into the needle's hub becomes less noticeable.

Once the needle is correctly positioned in the left cardiac ventricle, inject the cell suspension slowly into the left ventricle being careful not to move the needle or press it deeper into the thoracic cavity. Keep a close eye on the cell suspension in the syringe and do not inject the air bubble at the top of the syringe (**Figure 2b**). As soon as the cells have been inoculated, quickly remove the needle, apply slight pressure at the injection site for a few seconds and place the mouse on a heating pad until fully awake. Once mice have fully recovered, monitor their behavior for 24 h and watch for potential signs of embolism or distress.

Materials for intra-cardiac inoculation

(1) Anesthetized mouse (immune compromised if using human cells)
(2) Cellular suspension
(3) 0.5–1 cc insulin syringe, 27–29G, 0.5 inch
(4) Surgical tape
(5) Betadine and alcohol swabs
(6) Permanent marker
(7) Water recirculating heating pad

Intra-arterial inoculation of breast cancer cells in the tail. Once a mouse has been anesthetized with isoflurane, place it on a sterile surface in supine position and tape the torso of the mouse to the table for

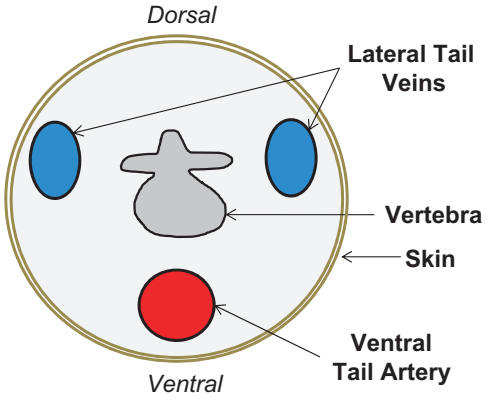

Figure 3 Schematic representation of the tail vasculature of a mouse.

stability. Use a heating pad or lamp to dilate the vessels within the tail for 2–3 min in order to facilitate greater ease of inoculation. Alternatively, the tail can be placed in warm water (30–35 °C). Using an alcohol pad, disinfect the tail vigorously, which will also help dilate the vessels within the tail and facilitate inoculation. Keep the tail clinched between the forefinger and thumb and insert the needle (beveled edge facing up) horizontally across the proximal section of the tail into the artery (**Figure 3**). Once the needle has entered the artery, the opposite hand is used to retract the syringe plunger slightly to inspect for a tight fitting within the artery and inspect the barrel of the syringe for a small amount of blood, which should appear at the needle hub. This will not occur if the needle has not breached the epithelial membrane of the artery or if the syringe has protruded through the artery. Once the syringe is properly

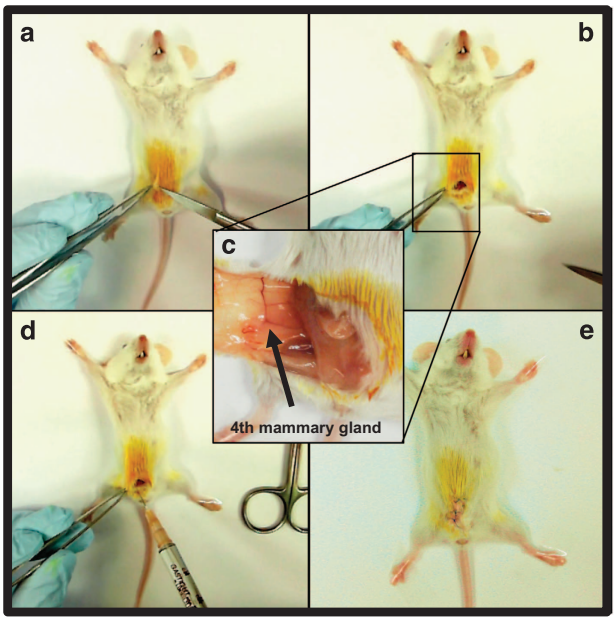

Figure 4 Inoculation of breast cancer cells in the 4th mammary fat pad of a mouse. (**a**, **b**) Place an anesthetized mouse in supine position on a sterile surface and tape the forelimbs and hind limbs away from the torso. Prior to inoculation, clean the inguinal surface of the animal thoroughly with betadine and alcohol. Using sterile surgical instruments, create a small incision in the skin adjacent to the 4th mammary fat pad. (**c**, **d**). Insert the needle into the fourth mammary gland fat pad and slowly inoculate the tumor cell suspension. The fourth mammary gland fat pad is located at the intersection of three prominent blood vessels. (**e**) After the injection of cells, close the wound with 4–6 sutures, administer an analgesic as per institutional guidelines and place the mouse on a heating pad until fully awake.

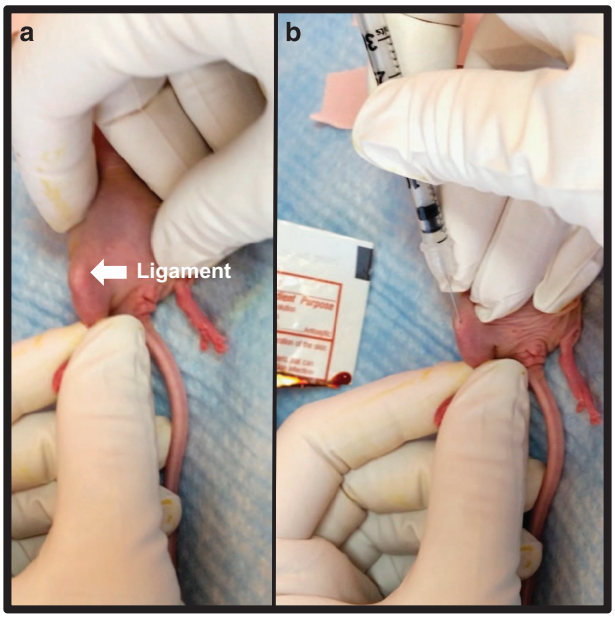

Figure 5 Inoculation of breast cancer cells in the proximal tibia of a mouse. (**a**) After sterilizing the hind limbs of an anesthetized mouse, bend the knee to nearly 90°. While holding the hind limb between the thumb and index finger, locate the patellar ligament between the knee and the tibia, which should be visible through the skin as a white longitudinal structure. (**b**) Holding the needle parallel to the tibia in the dominant hand, push the needle through the center of the patellar ligament and into the proximal end of the tibia. Resistance will be felt once the needle reaches the bone. Twist the needle slightly to drill through the growth plate until the needle can be felt giving way. Once inserted into the bone approximately 2–3 mm, inject the cell suspension slowly and then withdraw the needle using the same drilling motion used to enter the bone.

seated within the artery, depress the plunger slowly in order to minimize cell lysis resulting from fluid shear. The needle should ideally pierce the artery just once in order for the cell bolus to be delivered in its entirety. However, when small adjustments are futile, remove the needle completely and reposition the insertion point proximally to the initial site of injection. Once mice have fully recovered, monitor their behavior for 24 h and watch for potential signs of embolism, pain, or distress.

Materials for intra-arterial tail inoculation

(1) Anesthetized mouse (immune compromised if using human cells)
(2) Cellular suspension
(3) 0.5–1 cc insulin syringe, 27–29G, 0.5 inch
(4) Surgical tape
(5) Betadine and alcohol swabs
(6) Water recirculating heating pad

Orthotopic (mammary fat pad) inoculation of breast cancer cells. Place an anesthetized mouse in supine position on a sterile surface and tape the forelimbs and hind limbs away from the torso (**Figure 4a**). Prior to inoculation, clean the inguinal surface of the animal thoroughly with betadine and wipe with an alcohol pad or as per the institutional standard operating procedures. Using sterile surgical instruments, create a small incision in the skin adjacent to the fourth mammary fat pad (**Figures 4b and c**). Insert the needle into the fourth mammary gland fat pad and slowly inoculate the tumor cell suspension (**Figures 4d and e**; Supplementary Video 1). The 4th mammary gland fat pad is located at the intersection of three prominent blood vessels (**Figure 4c**). As with all techniques, it may be important for investigators to practice and familiarize themselves with the necessary anatomical landmarks prior to initiation of a multi-animal study. After the injection of cells, close the wound with 4–6 unconnected sutures, administer an analgesic as per institutional guidelines and place the mouse on a heating pad until fully awake.

In order to limit the occurrence of spontaneous tumor metastases to the lungs when using murine-derived cells (for example, 4T1), primary tumors can be surgically resected from anesthetized mice when tumors reach ~1 cm^3. Animals can then be followed for 3–4 additional weeks for the development of bone metastases.

Some laboratories have reported that orthotopic implantation of the human-derived breast cancer cell lines SUM-1315 and MDA-MB-231-IV into immune-compromised mice can elicit spontaneous metastasis to bone when preceded by engraftment of human bone plugs.[22,23] In this model, 5 mm bone biopsy cores obtained from human femoral heads (within 2–4 h of removal from the patient) can be implanted under the skin on the posterior surface of the animal prior to tumor cell inoculation in the mammary fat pad. Four weeks after bone plug implantation, the human bone grafts become vascularized and bone marrow resembles that of normal bone.[22,23] Orthotopic injection of human-derived tumor cells can then proceed as described, and the human bone plugs are then excised at the termination of the study (~8–14 weeks) and evaluated for the presence of breast cancer metastases.

Materials for orthotopic inoculation

(1) Anesthetized mouse (immune compromised if using human cells)
(2) Cellular suspension
(3) 0.1 cc Hamilton syringe, 25–27G, 0.5 inch
(4) Tape
(5) Betadine and alcohol swabs
(6) Sterile scissors and forceps
(7) Suture
(8) Water recirculating heating pad
(9) Analgesic

Intra-tibial inoculation of breast cancer cells. Prepare a syringe with the desired tumor cell suspension and set aside until ready to inject. After sterilizing the hind limbs, bend the knee to nearly 90° (**Figure 5a**). While holding the hind limb between the thumb and index finger, locate the patellar ligament between the knee and the tibia, which should be visible through the skin as a white longitudinal structure. Some laboratories choose to make a 2–3 mm incision through the skin on the knee to more easily visualize the tibia and patellar ligament; however, with practice this may not be necessary. Holding the needle parallel to the tibia in the dominant hand, push the needle through the center of the patellar ligament and into the proximal end of the tibia (**Figure 5b**). Resistance will be felt once the needle reaches the bone. Twist the needle slightly to drill through the growth plate until the needle can be felt giving way. Once inserted into the bone ~2–3 mm, attempt to move the needle slightly from side to side. When the needle is in the tibia, it will not be easily moved. If it moves freely from side to side, the needle is most likely embedded primarily in muscle and the insertion will need to be repeated. When the needle is accurately placed inside the marrow cavity of the tibia, inject the cell suspension slowly and then withdraw the needle using the same drilling motion used to enter the bone. In the event that the needle becomes clogged when penetrating or drilling through the top of the tibia, remove the original needle and re-insert a new needle, trying to follow the route created by the first needle. Once complete, use the same technique to inject the contralateral tibia with sterile PBS or desired vehicle to serve as a sham control. Bleeding rarely occurs; however, if blood does appear, apply pressure at the site. Administer an analgesic as per institutional guidelines, place the mouse on a heating pad and monitor until active.

Although cells can be inoculated into the tibia at any age, it is more difficult to penetrate the tibia in older animals once the growth plates have mineralized (>8-week old). On the other hand, very young mice can present injection difficulties due to the small size of the tibia; most laboratories therefore select 4- to 6-week-old mice for the intra-tibial inoculation route. If the mouse strain selected is furred, shave or wet the hair on the hind limb prior to the inoculation in order to better visualize the patellar ligament and other landmarks in the knee.

Materials for intra-tibial inoculation

(1) Anesthetized mouse (immune compromised if using human cells)
(2) Cellular suspension
(3) 0.1 cc Hamilton syringe, 25–27G, 0.5 inch
(4) Betadine and alcohol swabs
(5) Water recirculating heating pad
(6) Analgesic

Assessment of tumor progression in bone

Throughout a bone metastasis experiment, mice should be monitored daily for changes in activity levels, mobility and onset of cachexia, which is a paraneoplastic syndrome characterized in mice by loss of body weight, muscle atrophy and weakness, arched appearance and lethargy.[32,33] Mice should be euthanized when >10–20% body weight is lost, tumor progression impairs mobility (for example, long bone fracture, head-tilt, paraplegia) or an animal appears to be in respiratory distress. A subset of mice may require euthanasia sooner than other mice in large studies. With the exception of survival studies, it is important that mice be euthanized on the same day or as close to the same day as possible such that the experimental time frame is identical for all mice, thus permitting an accurate comparison of tumor progression between groups.

Osteolytic lesion area and abnormal bone remodeling can be visualized and assessed weekly *in vivo* using a cabinet X-ray machine (**Figure 6a**; **Table 4**). Because X-ray analysis is an assessment of overt osteolytic lesion formation and provides only indirect information on tumor cell growth, cancer cell lines are commonly transfected with bioluminescent proteins permitting *in vivo* visualization and quantitation of tumor growth at metastatic sites using bioluminescence imaging (BLI; **Table 4**).[11,20,34] BLI serves as an ideal complement to X-ray analysis of osteolysis, as it provides information on the presence of extra-skeletal metastases as well as micrometastases in bone, which precede bone destruction. Although not utilized to quantitate skeletal tumor burden, intra-vital microscopy may be useful for studying individual tumor cell motility and behavior in the bone microenvironment.[35]

At the termination of the study, mice should be subjected to necropsy and examined closely for gross evidence of metastatic foci outside of bone. For an intra-cardiac tumor inoculation study, evidence of tumor growth in the mediastinum surrounding the heart indicates that tumor cells were not accurately injected into the left cardiac ventricle, and the mouse should be excluded from the study. Fix all vital organs for future analysis. Carefully cut and scrape away skeletal muscle from the forelimbs, hind limbs and vertebral column, and fix the skeletal samples. Prior to decalcification of the bones, high-resolution *ex vivo* bone microcomputed tomography (μCT) can be performed to assess osteolytic or osteoblastic bone destruction and BV/TV at the distal femur, proximal tibia or lumbar vertebrae (**Figure 6b**).

Following decalcification, paraffin-embedded bone should be sectioned and stained with hematoxylin/eosin (H&E), and tumor burden (mm^2) should be measured in long bones and spine using image analysis software (**Figure 6c**). Osteoblast numbers may also be quantitated in H&E stained sections. Histological sections should also be stained for tartrate-resistant acid phosphatase activity in order to assess the total osteoclast number relative to the bone surface and the osteoclast number at the bone and tumor interface, all of which are known to increase with cancer-induced osteolysis (**Figure 6d**; **Table 4**).[36–37] Finally, serum can be assayed for the presence of bone turnover markers, hormones, inflammatory factors or growth factors of interest.

When applicable, quantification of spontaneous metastases to lung, liver, brain or adrenals can be performed in paraffin-embedded organs collected at necropsy. For these analyses, 5 μm sections can be cut every 200 μm through the organ and stained with H&E. The number and area of metastatic foci for each section can then be determined using image analysis software, and results can be expressed as the total metastatic foci number per organ and as total metastatic area per organ.

Discussion

When considering skeletal metastasis models with the intention of studying breast cancer osteolysis, a common choice is the intra-cardiac injection of human breast cancer cells in immune-compromised mice.[38–40] Alternatively, these human cells can be directly implanted into bone, bypassing earlier steps in the metastatic process. A benefit of the former model is that tumor cells detected in bone have themselves 'seeded the soil,' thus replicating the more natural progression of disseminated tumor cells formation of micrometastases, which progress in size over time, as occurs in humans. The necessity of using immune cell-deficient mice when inoculating human cell lines is typically seen as a limitation because it does not accurately model the immune competent human patient. It can, however, be seen as an advantage, as it eliminates possible confounding effects related to the animal's immune response and permits the study of human cells in a very permissive host environment.

The pathogenesis of breast cancer bone destruction in the intra-cardiac MDA-MB-231 model is relatively similar to the human condition. Upon inoculation, breast cancer cells circulate in the vasculature, home to the bone compartment, and micrometastases can be detected by BLI in distant skeletal sites in as early as 1 week after injection.[41] As the tumor cells proliferate in the bone microenvironment, tumor-derived

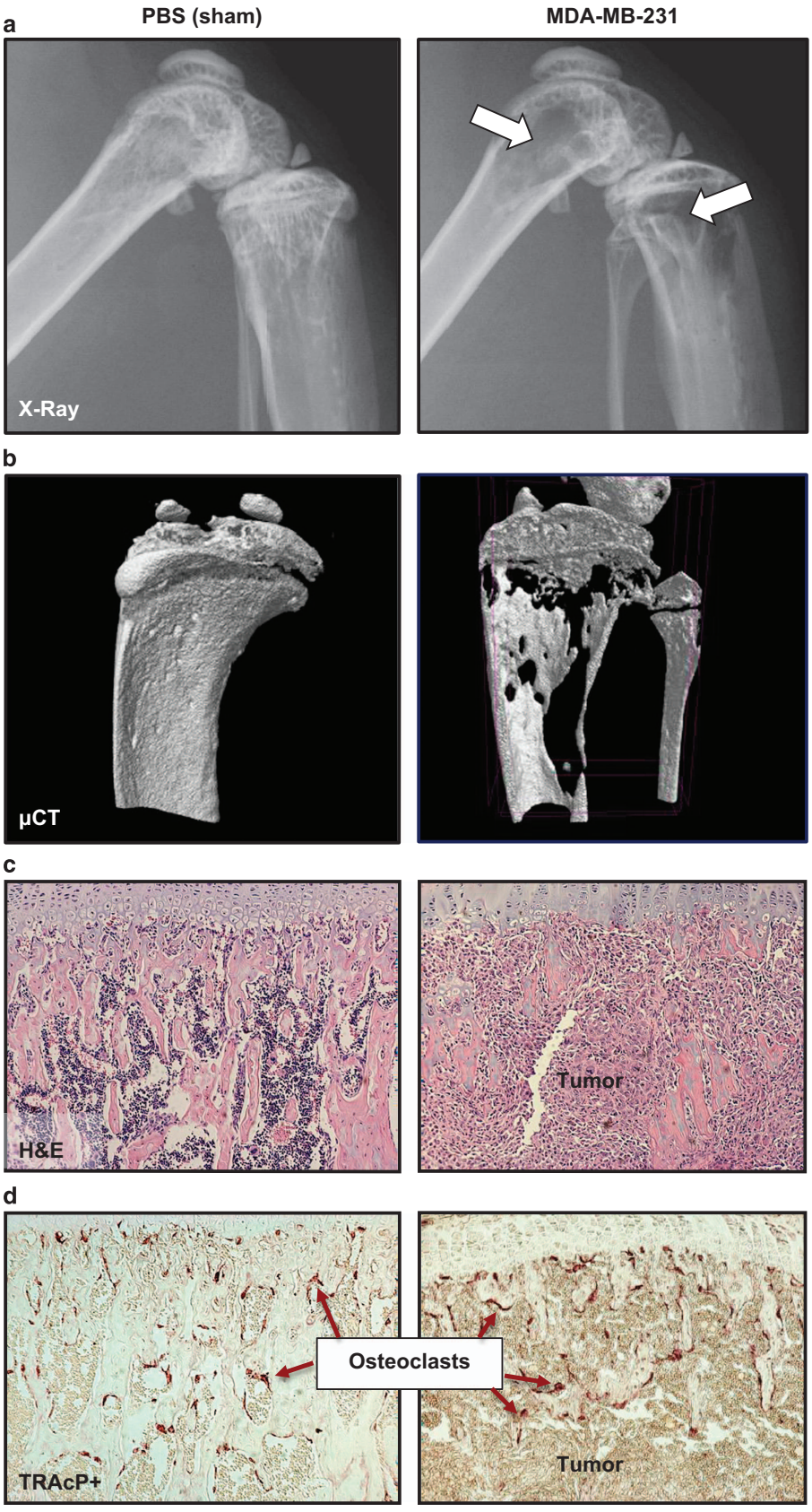

Figure 6 The assessment of tumor progression in bone can be carried out by (**a**) quantitation of osteolytic lesion area by X-Ray, (**b**) measurement of bone volume fraction (BV/TV) by bone high-resolution microcomputed tomography (μCT), (**c**) histological assessment of tumor area using hematoxylin/eosin (H&E) staining of long bones and vertebrae and (**d**) quantitation of tartrate-resistant acid phosphatase (TRAcP) + osteoclasts.

Table 3 Preparation of breast cancer tumor cells for inoculation in mice

Inoculation route	*Cell number*	*Volume (PBS)*	*Syringe/needle*
Intra-cardiac	100 000	100 μl	0.5–1 cc insulin/27–29G, 0.5 inch
Intra-arterial (tail)	100 000	100 μl	0.5–1 cc insulin/7–29G, 0.5 inch
Orthotopic	100 000–5 00 000	10–20 μl	0.1 cc Hamilton/25–27G, 0.5 inch
Intra-tibial	10 000–2 50 000	10–20 μl	0.1 cc Hamilton/25–27G, 0.5 inch

Table 4 Principal end points used to characterize the development of bone metastases in mice

Type	*Frequency*
In vivo analyses	
Activity levels and hind limb mobility	Daily
Respiratory distress	Daily
Symptoms of cachexia	Daily
X-ray analysis of osteolytic lesions	Weekly or bi-monthly
Bioluminescence imaging (BLI; if applicable)	Weekly or bi-monthly

Type	*Endpoint*
Post-mortem analyses	
Gross dissection	Inspection for visceral metastases in lung, liver, adrenals and brain tissue
Bone microcomputed tomography (μCT)	Trabecular bone volume/total volume (BV/TV) of the proximal tibia, distal femur and lumbar vertebrae
Histomorphometric analysis of bone	Tartrate-resistant acid phosphatase (TRAcP) staining of bone Osteoclast number/bone surface (OcN/BS) Osteoclast surface/bone surface (OcS/BS) Osteoclast number at the bone–tumor interface Hematoxylin/eosin (H&E) staining of bone for BV/TV and osteoblast number/bone surface (ObN/BS)
Tumor characterization	H&E staining of forelimbs, hind limbs and spine for total tumor area in bone Immunohistochemical staining for proteins of interest (e.g., cytokeratin, phospho-smads) H&E staining of visceral organs for quantitation of soft tissue metastases
Serum factors	Biomarkers, if applicable (e.g., bone turnover markers, hormones, inflammatory factors, growth factors, tumor-derived factors)

osteolytic factors stimulate osteoclastic bone resorption and the development of bone lesions, which are quantifiable by X-ray. The most substantial bone destruction tends to occur in the metaphyses of the distal femur and proximal tibia, likely due to the high vascularization and metabolic activity characteristic of these trabecular bone compartments.[42]

Estrogen receptor (ER)+ MCF-7 cells and triple negative MDA-MB-231 cells are two of the most commonly studied human breast cancer cell lines.[40] Although ER+ primary tumors have a high propensity to metastasize to bone in patients,[43] ER+ MCF-7 cells are utilized less frequently in models of breast cancer bone metastasis, as tumor-take can be limited using the intra-cardiac inoculation route, and MCF-7 cells require a longer time to develop osteolytic and osteoblastic lesions.[44,45] In contrast, ER− MDA-MB-231 cells readily metastasize to bone and develop osteolytic lesions as early as 2–3 weeks post inoculation.[39] In defense of the use of an ER− cell line, it should also be noted that there is a large discordance between the ER status of primary tumors and the ER status of the bone metastatic tumors in patients.[43]

The intra-tibial inoculation method is ideal for modeling the final stages of breast cancer bone metastasis and for studying direct interactions between tumor cells and the bone microenvironment without concerns about differential tumor-take from animal to animal. Murine-derived 4T1 cell proliferation in the tibia and subsequent development of osteolytic lesions can occur with the injection of as few as 10 000 murine-derived cells. At higher cellular concentrations (50 000–200 000 cells), our laboratories have observed 4T1 cell metastasis to contralateral tibiae, femurs, forelimbs and the lungs, often limiting the duration and utility of the model. As with all techniques presented here, it is recommended that investigators thoroughly characterize their cell line and inoculation route of choice by conducting dose–response studies in order to establish the optimal protocols prior to embarking on large animal trials.

Inoculation of cancer cells into the tail vein is a well-established bone metastasis model for multiple myeloma.[46,47] Our laboratories and others have found that the injection of breast cancer cells into the tail vein results almost exclusively in lung metastases, with limited tumor-take in bone.[22,48] When skeletal metastases are desired, we therefore recommend utilization of the tail artery as the tumor inoculation route for breast cancer models.[22,48–52]

In addition to specific limitations related to model choice discussed above, standard methodologies used by bone metastasis researchers to assess bone destruction and tumor burden have their own limitations. Osteolytic lesion area and tumor burden area in bone are typically assessed by measurement of X-Ray scan or by serial histological sectioning, respectively, and are thus merely two-dimensional approximations of three-dimensional tumors. Improvement in imaging has enhanced sensitivity of detection and yields more accurate

quantification of metastases. Typically, BLI using codon-optimized luciferase-labeled cells yields higher detection than fluorescent imaging using GFP-labeled cells.[53] Small animal imaging of bone has forged ahead with the development of high-resolution *in vivo* μCT scanners[54] in combination with BLI.[55] However, the bone metastasis research community has been slower to adopt such methodologies. One reason for this is that cumulative radiation exposure from CT scanners has been found to enhance metastases[56] and thus could confound cancer metastasis models if radiation exposure is not monitored judiciously.

Despite their limitations and caveats, the established murine models of breast cancer bone metastases have proven to be excellent tools for the study of bone and cancer cross talk and for the evaluation of potential therapeutics that prevent cancer progression and disrupt the cycle of bone destruction driven by metastasis.

Multimedia

The following article documents and visually demonstrates intra-cardiac and intra-tibial inoculation of cancer cells in mice and also demonstrates representative experimental end points of bone metastasis: http://www.jove.come/video/4260.

Conflict of Interest

The authors declare no conflict of interest.

Acknowledgements

We thank Alyssa Merkel and Kristin Kwakwa for capturing the photographs in **Figures 2 and 5** and Johnny Ribeiro and Khalid Mohammad for their technical input on the orthotopic and intra-tibial models, respectively. This work was supported by the Department of Defense Breast Cancer Research Program BC134025 (LEW) and by grants from INSERM (OP), the Comité Départemental de la Loire de la Ligue Contre le Cancer (OP), the Fondation ARC (OP), NIAMS AR43498 (GMP), The Netherlands Organization for Scientific Research NWO, VENI-Grant, 916.131.10 (JTB), the Department of Veterans Affairs 1I01BX001957 (JAS) and NCI 1R01CA163499 (JAS). Supported by the IBMS-ECTS Young Investigators.

References

1. Coleman RE. Skeletal complications of malignancy. *Cancer* 1997; **80**: 1588–1594.
2. Mundy GR. Metastasis to bone: causes, consequences and therapeutic opportunities. *Nat Rev Cancer* 2002; **2**: 584–593.
3. Thompson DD, Simmons HA, Pirie CM, Ke HZ. FDA Guidelines and animal models for osteoporosis. *Bone* 1995; **17**: S125–S133.
4. Ottewell PD, Wang N, Brown HK, Reeves KJ, Fowles CA, Croucher PI *et al.* Zoledronic acid has differential antitumor activity in the pre- and postmenopausal bone microenvironment *in vivo*. *Clin Cancer Res* 2014; **20**: 2922–2932.
5. Ottewell PD, Wang N, Brown HK, Fowles CA, Croucher PI, Eaton CL *et al.* OPG-Fc inhibits ovariectomy-induced growth of disseminated breast cancer cells in bone. *Int J Cancer* 2015; **137**: 968–977.
6. Lee JH, Kim B, Jin WJ, Kim JW, Kim HH, Ha H *et al.* Trolox inhibits osteolytic bone metastasis of breast cancer through both PGE2-dependent and independent mechanisms. *Biochem Pharmacol* 2014; **91**: 51–60.
7. Werbeck JL, Thudi NK, Martin CK, Premanandan C, Yu L, Ostrowksi MC *et al.* Tumor microenvironment regulates metastasis and metastasis genes of mouse MMTV-PymT mammary cancer cells *in vivo*. *Vet Pathol* 2014; **51**: 868–881.
8. Pécheur I, Peyruchaud O, Serre CM, Guglielmi J, Voland C, Bourre F *et al.* Integrin alpha(v)beta3 expression confers on tumor cells a greater propensity to metastasize to bone. *FASEB J* 2002; **16**: 1266–1268.
9. Ottewell PD, Deux B, Mönkkönen H, Cross S, Coleman RE, Clezardin P *et al.* Differential effect of doxorubicin and zoledronic acid on intraosseous versus extraosseous breast tumor growth *in vivo*. *Clin Cancer Res* 2008; **14**: 4658–4666.
10. Kang Y, Siegel PM, Shu W, Drobnjak M, Kakonen SM, Cordón-Cardo C *et al.* A multigenic program mediating breast cancer metastasis to bone. *Cancer Cell* 2003; **3**: 537–549.
11. Wetterwald A, van der Pluijm G, Que I, Sijmons B, Buijs J, Karperien M *et al.* Optical imaging of cancer metastasis to bone marrow: a mouse model of minimal residual disease. *Am J Pathol* 2002; **160**: 1143–1153.
12. Nutter F, Holen I, Brown HK, Cross SS, Evans CA, Walker M *et al.* Different molecular profiles are associated with breast cancer cell homing compared with colonisation of bone: evidence using a novel bone-seeking cell line. *Endocr Relat Cancer* 2014; **21**: 327–341.
13. Nasrazadani A, Van Den Berg CL. c-Jun N-terminal kinase 2 regulates multiple receptor tyrosine kinase pathways in mouse mammary tumor growth and metastasis. *Genes Cancer* 2011; **2**: 31–45.
14. Fathers KE, Bell ES, Rajadurai CV, Cory S, Zhao H, Mourskaia A *et al.* Crk adaptor proteins act as key signaling integrators for breast tumorigenesis. *Breast Cancer Res* 2012; **14**: R74.
15. Ottewell PD, Woodward JK, Lefley DV, Evans CA, Coleman RE, Holen I. Anticancer mechanisms of doxorubicin and zoledronic acid in breast cancer tumor growth in bone. *Mol Cancer Ther* 2009; **8**: 2821–2832.
16. Aslakson CJ, Miller FR. Selective events in the metastatic process defined by analysis of the sequential dissemination of subpopulations of a mouse mammary tumor. *Cancer Res* 1992; **52**: 1399–1405.
17. Abdelaziz DM, Stone LS, Komarova SV. Osteolysis and pain due to experimental bone metastases are improved by treatment with rapamycin. *Breast Cancer Res Treat* 2014; **143**: 227–237.
18. Lelekakis M, Moseley JM, Martin TJ, Hards D, Williams E, Ho P *et al.* A novel orthotopic model of breast cancer metastasis to bone. *Clin Exp Metastasis* 1999; **17**: 163–170.
19. Withana NP, Blum G, Sameni M, Slaney C, Anbalagan A, Olive MB *et al.* Cathepsin B inhibition limits bone metastasis in breast cancer. *Cancer Res* 2012; **72**: 1199–1209.
20. Buijs JT, Matula KM, Cheung H, Kruithof-de Julio M, van der Mark MH, Snoeks TJ *et al.* Spontaneous bone metastases in a preclinical orthotopic model of invasive lobular carcinoma; the effect of pharmacological targeting TGFβ receptor I kinase. *J Pathol* 2015; **235**: 745–759.
21. Iorns E, Drews-Elger K, Ward TM, Dean S, Clarke J, Berry D *et al.* A new mouse model for the study of human breast cancer metastasis. *PLoS ONE* 2012; **7**: e47995.
22. Kuperwasser C, Dessain S, Bierbaum BE, Garnet D, Sperandio K, Gauvin GP *et al.* A mouse model of human breast cancer metastasis to human bone. *Cancer Res* 2005; **65**: 6130–6138.
23. Holen I, Nutter F, Wilkinson JM, Evans CA, Avgoustou P, Ottewell PD. Human breast cancer bone metastasis *in vitro* and *in vivo*: a novel 3D model system for studies of tumour cell-bone cell interactions. *Clin Exp Metastasis* 2015; **32**: 689–702.
24. Suva LJ, Washam C, Nicholas RW, Griffin RJ. Bone metastasis: mechanisms and therapeutic opportunities. *Nat Rev Endocrinol* 2011; **7**: 208–218.
25. Engel LW, Young NA, Tralka TS, Lippman ME, O'Brien SJ, Joyce MJ. Establishment and characterization of three new continuous cell lines derived from human breast carcinomas. *Cancer Res* 1978; **38**: 3352–3364.
26. Engel LW, Young NA. Human breast carcinoma cells in continuous culture: a review. *Cancer Res* 1978; **38**: 4327–4339.
27. Soule HD, Vazguez J, Long A, Albert S, Brennan M. A human cell line from a pleural effusion derived from a breast carcinoma. *J Natl Cancer Inst* 1973; **51**: 1409–1416.
28. Levenson AS, Jordan VC. MCF-7: the first hormone-responsive breast cancer cell line. *Cancer Res* 1997; **57**: 3071–3078.
29. Yi B, Williams PJ, Niewolna M, Wang Y, Yoneda T. Tumor-derived platelet-derived growth factor-BB plays a critical role in osteosclerotic bone metastasis in an animal model of human breast cancer. *Cancer Res* 2002; **62**: 917–923.
30. Thomas RJ, Guise TA, Yin JJ, Elliott J, Horwood NJ, Martin TJ *et al.* Breast cancer cells interact with osteoblasts to support osteoclast formation. *Endocrinology* 1999; **140**: 4451–4458.
31. Canon J, Bryant R, Roudier M, Branstetter DG, Dougall WC. RANKL inhibition combined with tamoxifen treatment increases anti-tumor efficacy and prevent tumor-induced bone destruction in an estrogen receptor-positive breast cancer bone metastasis model. *Breast Cancer Res Treat* 2012; **135**: 771–780.
32. Fearon KC, Glass DJ, Guttridge DC. Cancer cachexia: mediators, signaling, and metabolic pathways. *Cell Metab* 2012; **16**: 153–166.
33. Waning DL, Mohammad KS, Reiken SR, Wenjun X, Anderssen DC, John S *et al.* TGFβ mediates muscle weakness associated with bone metastases. *Nat Med* 2015; **21**: 1262–1271.
34. Rucci N, Capulli M, Ventura L, Angelucci A, Peruzzi B, Tillgren V *et al.* Proline/arginine-rich end leucine-rich repeat protein N-terminus is a novel osteoclast antagonist that counteracts bone loss. *J Bone Miner Res* 2013; **28**: 1912–1924.
35. Ellenbroek SI, van Rheenen J. Imaging hallmarks of cancer in living mice. *Nat Rev Cancer* 2014; **14**: 406–418.
36. Guise TA. Molecular mechanisms of osteolytic bone metastases. *Cancer* 2000; **88**: 2892–2898.
37. Wright LE, Frye JB, Lukefahr AL, Timmermann BN, Mohammad KS, Guise TA *et al.* Curcuminoids block TGF-β signaling in human breast cancer cells and limit osteolysis in a murine model of breast cancer bone metastasis. *J Nat Prod* 2013; **76**: 316–321.
38. Arguello F, Baggs RB, Frantz CN. A murine model of experimental metastasis to bone and bone marrow. *Cancer Res* 1988; **48**: 6876–6881.
39. Guise TA, Yin JJ, Taylor SD, Kumagai Y, Dallas M, Boyce BF *et al.* Evidence for a causal role of parathyroid hormone-related protein in the pathogenesis of human breast cancer-mediated osteolysis. *J Clin Invest* 1996; **98**: 1544–1549.

40. Yoneda T, Sasaki A, Dunstan C, Williams PJ, Bauss F, De Clerck YA *et al.* Inhibition of osteolytic bone metastasis of breast cancer by combined treatment with the bisphosphonate ibandronate and tissue inhibitor of the matrix metalloproteinase-2. *J Clin Invest* 1997; **99**: 2509–2517.
41. Johnson LC, Johnson RW, Munoz SA, Mundy GR, Peterson TE, Sterling JA. Longitudinal live animal micro-CT allows for quantitative analysis of tumor-induced bone destruction. *Bone* 2011; **48**: 141–151.
42. Rosol TJ, Tannehill-Gregg SH, Corn S, Schneider A, McCauley LK. Animal models of bone metastasis. *Cancer Treat Res* 2004; **118**: 47–81.
43. Coleman RE, Rubens RD. The clinical course of bone metastases from breast cancer. *Br J Cancer* 1987; **55**: 61–66.
44. Rucci N, Ricevuto E, Ficorella C, Longo M, Perez M, Di Giacinto C *et al.* In vivo bone metastases, osteoclastogenic ability, and phenotypic characterization of human breast cancer cells. *Bone* 2004; **34**: 697–709.
45. Lu X, Wang Q, Hu G, Van Poznak C, Fleisher M, Reiss M *et al.* ADAMTS1 and MMP1 proteolytically engage EGF-like ligands in an osteolytic signaling cascade for bone metastasis. *Genes Dev* 2009; **23**: 1882–1894.
46. Dallas SL, Garrett IR, Oyajobi BO, Dallas MR, Boyce BF, Bauss F *et al.* Ibandronate reduces osteolytic lesions but not tumor burden in a murine model of myeloma bone disease. *Blood* 1999; **93**: 1697–1706.
47. Mitsiades CS, Mitsiades NS, Bronson RT, Chauhan D, Munshi N, Treon SP *et al.* Fluorescence imaging of multiple myeloma cells in a clinically relevant SCID/NOD in vivo model: biologic and clinical implications. *Cancer Res* 2003; **63**: 6689–6696.
48. Yang S, Zhang JJ, Huang XY. Mouse models for tumor metastasis. *Methods Mol Biol* 2012; **928**: 221–228.
49. van der Horst G, van der Pluijm G. Preclinical models that illuminate the bone metastasis cascade. In: Joerger M, Gnant M (eds). *Prevention of Bone Metastases*. Springer-Verlag: Berlin, Heidelberg, Germany, 2012, p. 1–24.
50. Buijs JT, Henriquez NV, van Overveld PG, van der Horst G, Que I, Schwaninger R *et al.* Bone morphogenetic protein 7 in the development and treatment of bone metastases from breast cancer. *Cancer Res* 2007; **67**: 8742–8751.
51. Bachelier R, Confavreux CB, Peyruchaud O, Croset M, Goehrig D, van der Pluijm G *et al.* Combination of anti-angiogenic therapies reduces osteolysis and tumor burden in experimental breast cancer bone metastasis. *Int J Cancer* 2014; **135**: 1319–1329.
52. Croset M, Goehrig D, Frackowiak A, Bonnelye E, Ansieau S, Puisieux A *et al.* TWIST1 expression in breast cancer cells facilitates bone metastasis formation. *J Bone Miner Res* 2014; **29**: 1886–1899.
53. Peyruchaud O, Winding B, Pécheur I, Serre CM, Delmas P, Clézardin P. Early detection of bone metastases in a murine model using fluorescent human breast cancer cells: application to the use of the bisphosphonate zoledronic acid in the treatment of osteolytic lesions. *J Bone Miner Res* 2001; **16**: 2027–2034.
54. Bouxsein ML, Boyd SK, Christiansen BA, Guldberg RE, Jepsen KJ, Müller R. Guidelines for assessment of bone microstructure in rodents using micro-computed tomography. *J Bone Miner Res* 2010; **25**: 1468–1486.
55. Lim E, Modi K, Christensen A, Meganck J, Oldfield S, Zhang N. Monitoring tumor metastases and osteolytic lesions with bioluminescence and micro CT imaging. *J Vis Exp* 2011; **50**: 2775.
56. Cowey S, Szafran A, Kappes J, Zinn KR, Siegal GP, Desmond RA *et al.* Breast cancer metastasis to bone: evaluation of bioluminescent imaging and microSPECT/CT for detecting bone metastasis in immunodeficient mice. *Clin Exp Metastasis* 2007; **24**: 389–401.

Supplementary Information accompanies the paper on the BoneKEy website (http://www.nature.com/bonekey)